In-plane structural anisotropy of ultrathin Fe films on GaAs(001)-4×6: X-ray absorption fine-structure spectroscopy measurements

R. A. Gordon and E. D. Crozier
Department of Physics, Simon Fraser University, Burnaby, British Columbia, Canada V5A 1S6
(Received 29 January 2006; revised manuscript received 14 August 2006; published 9 October 2006)

Iron films of thickness 2 monolayers (ML) and 5 monolayers prepared on pseudo 4×6-reconstructed GaAs(001) surfaces were studied *in situ* at the PNC/XOR beamline by polarization-dependent x-ray absorption fine structure methods to investigate structural anisotropy in the plane of the films and compare with theoretical predictions. These two thicknesses are on either side of the transition from island to layer-by-layer growth modes and provide insight into possible structural origins of in-plane uniaxial magnetic anisotropy observed in this magnetic film system. First-principles calculations by [Mirbt *et al.*, Phys. Rev. B **67**, 155421 (2003)] have suggested a splitting in the nearest neighbor distances of the iron could be as large as 0.06 Å, for 1 ML of arsenic having migrated to the film surface, distorting the structure slightly from body-centered tetragonal along the ⟨110⟩ and ⟨−110⟩ directions. We observe a splitting of approximately 0.02(1) Å at 2 ML in the nearest-neighbor distances. An electronic anisotropy was detected at 2 ML that could correspond to differences in bonding between gallium and arsenic dangling bonds. An anisotropy in mean-square relative displacement was apparent for the 5 ML film, though no difference in nearest-neighbor distances was observed beyond error.

DOI: 10.1103/PhysRevB.74.165405 PACS number(s): 68.55.Jk, 75.70.Ak, 75.30.Gw, 61.10.Ht

I. INTRODUCTION

Thin films of iron on single-crystal gallium arsenide semiconducting substrates provide an intriguing system for the development of new magnetoelectronic devices.[1–10] Use of the (001)-oriented substrate, with several reconstruction choices providing arsenic or gallium-rich surface termination, has enabled epitaxial growth of iron films.[11–14] In-plane magnetic anisotropy measurements on thin films of Fe on GaAs have revealed a fourfold component[15–17] consistent with a body-centered tetragonally distorted iron (observed for thin films on 4×6 reconstructed surface[18,19]) or cubic iron along an (001) axis. With decreasing film thickness, a uniaxial component to the in-plane magnetic anisotropy also becomes apparent,[15–17,20–24] increasing in strength with decreasing thickness.

The origin of this uniaxial magnetic anisotropy (UMA) is attributed to the Fe-GaAs interface. It produces an easy axis along the substrate ⟨110⟩ direction, independent of surface reconstruction.[11,12,14,15,21] Bonding (Fe-As) at the interface has been considered the likely source for this UMA.[16,22,23,25] Theoretical calculations by Mirbt *et al.*[26] have also suggested an anisotropic in-plane strain, differing along ⟨110⟩ and ⟨−110⟩, as a contributing factor. This anisotropic strain suggests a structural distortion in plane. This would be in addition to the observed distortion of the out-of-plane direction of the film when compared to the in plane.[19] In this work we address a possible in-plane structural anisotropy in iron films epitaxially grown on the pseudo-4×6 reconstructed GaAs(001) [which is comprised of both 4×2 and 2×6 (Ref. 11) or 1×6 (Refs. 27 and 28) reconstructions] surface.

Iron growth on this GaAs(001) surface is marked by two regimes. Below 3–4 ML, iron grows as islands, with coalescence and pseudo-layer-by-layer growth occurring above 4 ML.[13] Arsenic has been observed to segregate to the surface during growth. To date, neither electron nor x-ray methods have confirmed the existence of an in-plane distortion, but studies at this low-coverage level focus more on island or domain size using STM or reflection high energy electron diffraction (RHEED) (Ref. 1) and it is possible that any distortion is small enough to be overlooked. An x-ray diffraction study,[22] in agreement with RHEED measurements, observed that a film of 1.5 nm thickness (approximately 10 ML) was pseudomorphic with the substrate—matching the lattice in plane. This was also concluded by polarization-dependent extended x-ray absorption fine structure (EXAFS) measurements[18,19] comparing in-plane to out-of-plane structure. The iron films could be fit to a body-centered tetragonal structure with a ratio $c/\langle a\rangle$ of 1.03, but the possibility of an in-plane distortion of the magnitude predicted by the first principles calculation of Mirbt *et al.* was not conclusively decided. Further examination of this system at low coverage is required.

The calculations by Mirbt *et al.*[26] were done for 0.5, 1, 2, and 5 monolayers (ML) of iron on gallium arsenide, at 0 K for no specific reconstruction of the surface. With 1 ML of As segregated at the surface, their results for the ratio of c-lattice to mean a-lattice constant ($c/\langle a\rangle$) and percentage in-plane contraction or expansion along ⟨110⟩ or ⟨−110⟩ are summarized in Table I for 2 and 5 ML. Also listed are calculated nearest-neighbor distances based on the theoretical in-plane contractions and out-of-plane expansion. The effects of this in-plane distortion on the nearby environment of a central absorbing atom are illustrated in Fig. 1. It should be noted that distortions along ⟨−110⟩ and ⟨110⟩ will affect the distances of all four in-plane second nearest-neighbors equally (but will change the angles between them). EXAFS, while an excellent probe of the local environment of an absorbing atom, lacks the ability to resolve such small splittings in near-neighbors as listed in Table I under typical experimental conditions.[29] The body-centered cubic [tetragonal by EXAFS (Ref. 19) or related orthorhombic if distorted in-plane] structure eases this problem when using a linearly-polarized x-ray beam from a synchrotron. Due to the dipole-

TABLE I. Theoretical predictions of an in-plane distortion in Fe films on GaAs after Mirbt *et al.* (Ref. 26) with a 1 ML arsenic overlayer, and the calculated effects on first nearest-neighbor distances.

Film	2 ML	5 ML	bcc Fe
% change ⟨110⟩	−2.79	−1.83	0
% change ⟨−110⟩	0.86	0.51	0
$c/\langle a\rangle$	1.05	1.03	1
1st n.n. ⟨110⟩/Å	2.471	2.472	2.482
1st n.n. ⟨−110⟩/Å	2.531	2.510	2.482

like distribution of the emitted photoelectron in the EXAFS process,[30–34] atoms perpendicular to the x-ray electric field vector contribute little to the EXAFS spectrum. By orienting the electric field vector along the ⟨110⟩ and ⟨−110⟩ directions of the substrate and film, as illustrated in Fig. 2, we can separate the nearest-neighbor atom contributions based on crystallographic direction. In this paper, we present polarization-dependent EXAFS measurements on 2 and 5 ML iron films on GaAs(001) with the pseudo-4×6 reconstruction. These films are on either side of the change in growth mode from island to layer-by-layer and allow us to measure directly the extent of any in-plane structural distortion near the interface of iron on GaAs(001).

II. EXPERIMENT

Samples of 2 and 5 monolayer thickness were prepared and measured *in situ* using the MBE1 end station at the PNC/XOR undulator beamline,[35] Sector 20 of the Advanced Photon Source. A custom sample-positioning system (Thermionics Northwest GB-16 based) permitted the epiready *n*-type GaAs substrates (American Xtal Technology) to be oriented anywhere from normal incidence to grazing angle for incident x rays, and with variable orientation in-plane

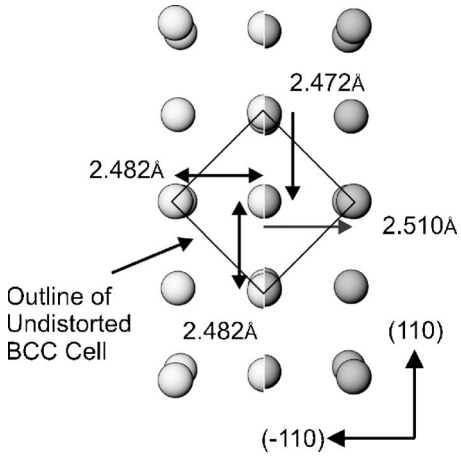

FIG. 1. Comparison of undistorted body-centered cubic iron (left) and the theoretical distortion (right) after Mirbt *et al.* (Ref. 26) for 5 monolayers of iron on GaAs with 1 monolayer of an arsenic overlayer.

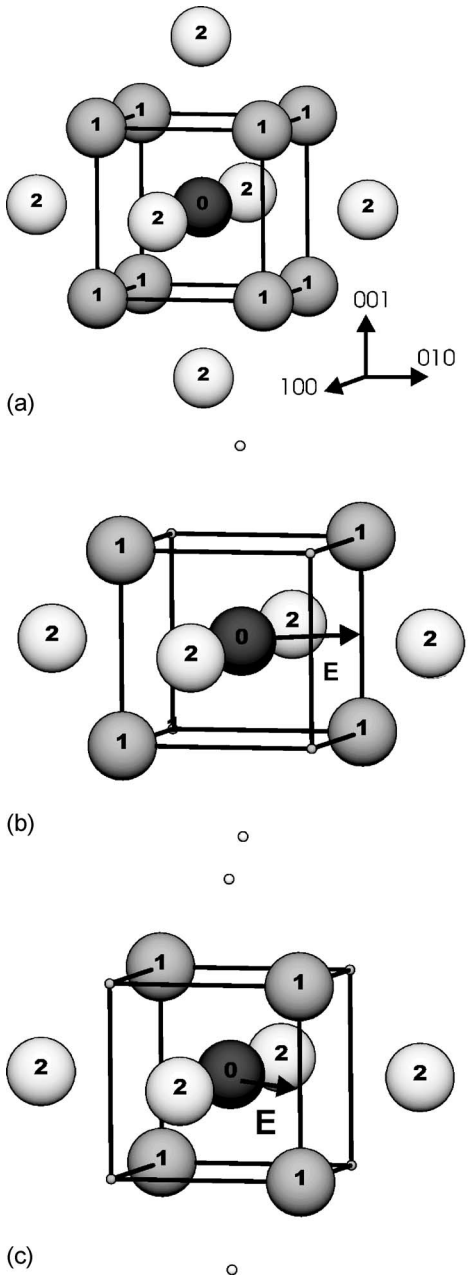

FIG. 2. The body-centered cubic structure from an XAFS perspective, with central atom "0", nearest neighbors "1" and next-nearest neighbors "2" as viewed with (a) unpolarized x rays; (b) x-rays polarized along ⟨−110⟩; and (c) polarized along ⟨110⟩.

(±110°, 2 arcsecond step size). Samples were introduced to the vacuum (base pressure 2×10^{-10} Torr), given a 1 h thermal desorption treatment at 600°C, then sputtered at room temperature for 3 h using 500 eV Ar^+ at a pressure of 2×10^{-5} Torr. Substrates were subsequently annealed and monitored by RHEED until ×4 and ×6 reconstructions were observed. This preparation method is similar to that used by Monchesky *et al.*[27,28] and has been shown by scanning-tunneling-microscopy (STM) to yield a mixed-reconstruction of 4×2 and 1×6. A mix of 4×2 and 2×6 has also been observed[11] when samples were sputtered at elevated temperatures. Samples for our XAFS study were not examined

by STM, but are likely to possess a mixed-phase surface reconstruction (pseudo-4×6). This may influence how the iron islands nucleate on the surface,[11,12] with a preference for elongation along the higher-order reconstruction direction. In these same works, this growth has been shown to have only a slight enhancement of the UMA for the 2×6 reconstruction over the 4×2. Evidence[11,14] suggests, however, that identical interfaces are formed, independent of reconstruction, but with the potential for differing amounts of arsenic to segregate to the film surface (owing to the more As-rich nature of the 2×6 reconstruction). Iron films for XAFS analysis were deposited using Omicron EFM3 evaporators at a rate of 1 ML/min at room temperature and also monitored by RHEED. Oscillations in the specular spot intensity (with sample angle set at the first anti-Bragg condition) of the electron beam were used to determine film thickness.

Fluorescence-mode x-ray measurements were made at the Fe *K* edge. The silicon (111) double-crystal monochromator on the PNC/XOR undulator line was detuned by 25% at 7500 eV to reduce harmonic energies in the x-ray beam. The x-ray beam was incident on the single-crystal substrates at approximately 2/3 of the critical angle ($\theta_c \sim 0.4^\circ$) for total reflection at 250 eV above the edge to avoid errors caused by anomalous dispersion.[30] The electric field vector of the x-rays was aligned to within this angle of the ⟨001⟩ direction for out-of-plane EXAFS measurements or within 2° of the ⟨−110⟩ or ⟨110⟩ orientations for in-plane measurements. Small azimuthal in-plane adjustments were made within this 2° margin to shift small Bragg peaks contaminating the fluorescence signal and facilitate the removal of these peaks during processing. For both the 2 ML and 5 ML samples, an argon-filled (1 atm), UHV compatible, fluorescence ionization chamber[36] was used to collect fluorescence data. A helium-filled (1 atm, flowing) parallel-plate ionization chamber was used to measure the incident x-ray intensity, I_0. An iron foil was also measured in transmission for analysis, then located in front of a reference detector[37] using scattered radiation for monitoring energy calibration during measurements of the films. A motorized set of Huber slits was used to set the beam size to approximately $70 \times 1000\ \mu m^2$ so that the footprint of the beam did not exceed the size of the substrates when at grazing angle.

III. RESULTS AND DISCUSSION

Figure 3 compares the x-ray absorption near edge spectra (XANES) for the in-plane polarization measurements of the 5 and 2 monolayer samples. Small differences do exist between the two orientations for both samples, but the differences predicted by theory are also small, so care must be taken in examining features as processing effects (small differences in background removal for example) and step size (0.5 eV) may obscure results. The overlapping first peaks in the derivatives, near 7110.7 eV indicate no noticeable edge shift (within one half step) between orientations, based on estimates of the centers of the two peaks which are both about 1.4 eV wide. For the 5 ML film, the XANES curves do not exhibit noticeable differences until above 7120 eV, with the peak near 7129 eV occurring 0.5 eV higher in energy for

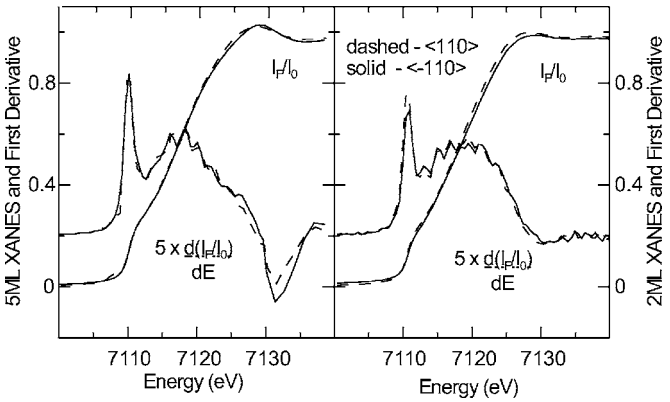

FIG. 3. Comparison of in-plane XANES spectra and first derivatives for 5 and 2 monolayer iron films on GaAs(001)-4×6. Fluorescence data, I_f, has been normalized to the incident x-ray intensity, I_0. Derivatives have been displaced upwards and rescaled for ease of view.

the ⟨−110⟩ direction. At this energy, one is entering the low-*k* (photoelectron momentum *k*) region of the extended XAFS spectrum, so differences may have a structural contribution stronger than any electronic effect, necessitating analysis of the EXAFS spectra before interpreting the results. Similarly, the 2 ML data exhibit differences throughout this energy range, with the peak near 7129 eV occurring 1 eV higher for the ⟨−110⟩ direction than for the ⟨110⟩. The 2 ML data also exhibit a small difference around the edge position. The peak in the derivative is smaller for the ⟨−110⟩ orientation. Since this region of the XANES involves Fe states at the Fermi level, this may be an indication of differences in bonding to the GaAs substrate between the two in-plane orientations. This may be due to differences in the orientations of Ga and As dangling bonds.[1]

The EXAFS spectra were extracted from the normalized fluorescence data using the program AUTOBK,[38] then averaged, and are shown in Fig. 4. Fourier transforms were taken with a 10% Gaussian window and k^2 weighting over the same ranges for a given thickness: 5 ML ~2.3 to 14Å^{-1}, 2 ML ~2.3−12Å^{-1}, and are shown in Fig. 5. Immediately apparent are the differences between the two in-plane orientations for the 5 ML film. The amplitude for the ⟨110⟩ orientation is smaller and the double-peak feature near 5Å^{-1} in Fig. 4 is less pronounced. There are a number of possible reasons for this. The layer size could be anisotropic. Diffraction work[22] on a 1.5 nm film (10 ML) found that the diffraction peak widths differed between the (−220) and (−2−20) reflections, with the (−2−20) reflection being considerably broader. This was attributed to differing domain sizes. The 5 ML film in our work is just above the transition from island to layer growth. It is possible that the islands have not coalesced fully, leaving more Fe atoms exposed and not fully coordinated. If the islands that formed early in the growth were anisotropic[11,12]—elongated along the ⟨−110⟩ direction—then the connectivity that occurred during coalescence may have preferred the ⟨−110⟩ direction, leaving the ⟨110⟩ poorly connected and hence, leaving Fe atoms undercoordinated at the edges of the islands/layers in that direc-

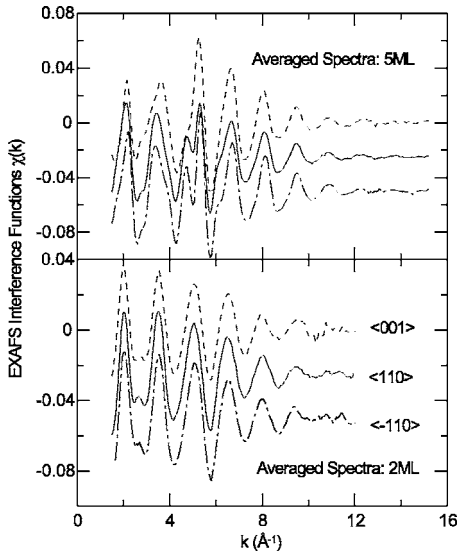

FIG. 4. Polarization-dependent EXAFS interference functions, $\chi(k)$, at the iron K edge for 2 and 5 monolayer films on GaAs(001)-4×6 with x-rays polarized along the ⟨001⟩, ⟨−110⟩, and ⟨110⟩ directions.

tion. Even though the surface is likely a mixture of reconstructions, both with a preferred growth direction,[11] it is possible that one of the reconstructions (containing the ×6 along ⟨−110⟩) is causing favored growth. Another possible reason would be increased disorder in the ⟨110⟩ direction. Fitting would be able to distinguish between these two scenarios, and is discussed below. Although a small difference in Fourier transform peak position seems evident for the 2 ML film, fitting is also required.

Data were fit in R space using a capped-film model that accounts for the presence of substrate atoms in the coordination spheres of the target iron atom as well as the reduction in coordination due to finite thickness as described elsewhere.[19,39] As with the theoretical calculations of Mirbt *et al.*,[26] this structural model is not dependent on surface reconstruction. A polarization-dependent model was generated using the program FEFF7 (Ref. 40) and nonlinear-least-squares fit to the data using a modified version of the XAFS equation:

$$\chi_{model}(k) = \sum \frac{S_0^2 N_j F_j(k)}{kR_j^2} e^{(-2k^2\sigma_j^2)} e^{(-2R_j/\lambda)} \sin[2kR_j + \delta_j(k)] \tag{1}$$

using the program WINXAS.[41] In this model equation, the polarization dependence to the scattered photoelectron intensity is included in the FEFF-calculated scattering amplitude, F_j, for the jth shell which has N_j equivalent atoms located at distance R_j and mean-square relative displacement σ_j^2 (with photoelectron mean-free-path λ and phase shift δ provided by FEFF). The term S_0^2 acts as an overall scaling factor. Since coordination numbers were fixed according to the model when fitting, S_0^2 also serves to indicate deviations in coordination from the model values. In addition to fitting S_0^2, R, and σ^2, a parameter for monitoring deviation between the FEFF-calculated band energy and the band structure in the actual films, ΔE_0, was also fit. Fit results are summarized in Table II. For the 5 ML film, both first and second near-neighbors could be fit under the primary peak in the Fourier transform. For the 2 ML film, only one peak could be fit in this area.

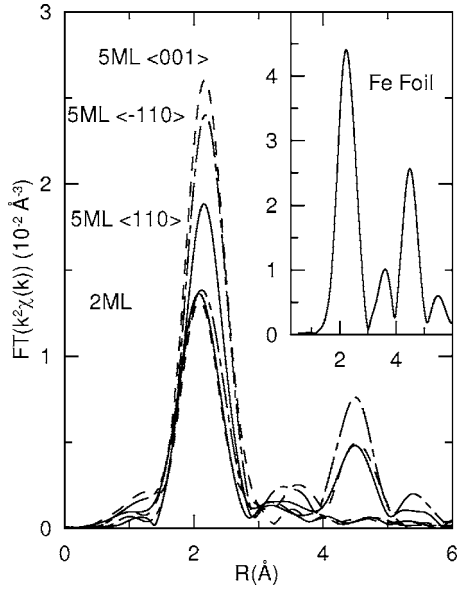

FIG. 5. Fourier transforms, with k^2 weighting, of the EXAFS interference functions of Fig. 4. Shown inset is the corresponding transform for an iron foil. Curve characteristics (solid line, dashed, or dash-dot) identifying polarization are as in Fig. 4.

Fit results for the 5 ML film appear straightforward and consistent with previous interpretations of XAFS data[18,19] as well as diffraction data for a 1.5 nm film.[22] Within error, both in-plane orientations yield the same results for near-neighbor distances. Indeed, since the 4 in-plane second nearest-neighbors should be at the same distance for both in-plane orientations [Figs. 2(b) and 2(c)] independent of any distortion along ⟨110⟩ or ⟨−110⟩, if the fit is repeated with R_2 constrained to be the same for both, then the small difference (again, within error) between the R_1 values diminishes to 0.002(10) Å. What, then, is the reason for the difference in the amplitudes of the XAFS interference functions? The S_0^2 values are comparable. This indicates that the average coordination of the iron atoms is comparable in both orientations, ruling out the poor connectivity of islands discussion above. The answer lies in the mean-square-relative-displacements (msrds), which differ greatly between the two in-plane orientations. This is an indication of greater disorder along the ⟨110⟩ direction—perhaps the result of preferred growth along the ⟨−110⟩ direction for the ×6 reconstructions. Preferred growth, however, is reconstruction-dependent and UMA is largely independent of reconstruction.

Interpretation of the 2 ML results also seems straightforward, but it is not. There is an apparent difference in nearest-neighbor distances of 0.02(1) Å between the ⟨110⟩ and ⟨−110⟩ directions, with the ⟨−110⟩ being larger, as predicted by the first-principles calculations of Mirbt *et al.*,[26] but the difference is smaller by a factor of 3. The msrds are comparable, so an anisotropic disorder term is less of a concern.

TABLE II. Fit for both 2 and 5 monolayer iron films on GaAs for out-of-plane and two in-plane polarizations.

Sample and polarization	R_1 (Å)	σ_1^2 (10^{-4} Å^2)	R_2 (Å)	σ_2^2 (10^{-4} Å^2)	ΔE_0 (eV)	S_0^2
bcc Fe	2.482		2.866			
Fe foil	2.474(6)	52(4)	2.852(9)	67(8)	5.6(7)	0.76(3)
5 ML ⟨001⟩	2.478(5)	68(3)	2.92(4)	159(40)	4.5	0.63
⟨110⟩	2.479(5)	73(3)	2.803(9)	168(20)	3.0	0.58
⟨−110⟩	2.473(5)	60(3)	2.815(9)	128(20)	3.7	0.59
2 ML ⟨001⟩	2.462(5)	108(5)			1.1	0.56
⟨110⟩	2.450(5)	110(5)			−0.7	0.63
⟨−110⟩	2.471(5)	112(5)			3.2	0.68

Scaling factors differ slightly beyond error, so some coordination number variations (i.e., anisotropic island size) may be present (elongated along ⟨−110⟩, consistent with preferred growth along the ×6 reconstruction) but the reduced out-of-plane S_0^2 suggests some differences in background removal and normalization may be affecting these values. The more startling difference arises from the difference in E_0 shift (ΔE_0). Care must be taken in interpreting differences in R when there are differences in ΔE_0 since these parameters can be correlated in fitting XAFS data. To see if this correlation was skewing the fit results, fits were attempted with ΔE_0 fixed to the out-of-plane value, 1.1 eV. While this did decrease the difference in in-plane R_1 values to 0.011(10) Å, the quality of the fits deteriorated substantially. The fit residual (magnitude of the difference between experimental data and calculated values from fit model, summed and divided by the sum of the magnitude of the experimental data, expressed as a percentage)[18,39] went from 1.2 to 5.0 for the ⟨110⟩ data, from 1.0 to 5.8 for the ⟨−110⟩ data, and visually, the simulated curves differed from the data. Correlation between parameters cannot be the cause of the apparent anisotropy in both R and ΔE_0 in-plane. The anisotropy must be real.

The model used for fitting is that of an infinite sheet of iron capped above and below by a layer of substrate atoms.[19] Since Ga and As are indistinguishable in backscattering from each other during an iron K-edge XAFS spectrum, the model treats them as the same and in FEFF, the element Ge was used to represent the average. The electronegativities of Ga and As are different. The orientations of the dangling As and Ga bonds differ in-plane. It is quite possible that the differences in R and E_0 shift are due to differences in the atoms to which the iron bonds on the substrate. This would give rise to differences in band structure that would be consistent with the small differences observed in the near edge spectra around 7111 eV. The effects of anisotropic bonding at the interface on the average iron environment can be expected to diminish with increasing film thickness and would be consistent with the lack of any significant distortion in neighbor distances for the 5 ML film. One cautionary note in considering these results from below island coalescence is that they are islands, not layers. They may not truly represent the first 2 ML of a thicker film. Marker studies, such as those done to look at magnetic behavior at the interface,[8–10] could provide a closer approximation to the interface for a thicker film.

At 2 ML, a small structural distortion is observed; at 5 ML one is not. It is possible that kinetic effects are playing a role since the XAFS measurements were done at room temperature while the calculated distortions[26] were for 0 K. There is also a postulated structural transition from amorphous to crystalline that may be influencing the behavior of these films.[14,21] The possibility of such a transition is supported by the absence of higher-order scattering paths in the in-plane XAFS data of the 2 ML sample—an indication of poor ordering. Such a transition (disordered to ordered) may explain the 20% increase in the uniaxial in-plane anisotropy constants observed[11] between 4 ML and 5 ML thickness (as the island coalesce). The anisotropic disorder observed in the XAFS of the 5 ML sample may be a remnant of this transition. If the origins of this anisotropic disorder lie in how the process of coalescence and increased-order resulted in relieving the structural distortion in the islands, then it could possess the same independence of reconstruction as the UMA, and hence contribute to the origin of the uniaxial magnetic anisotropy rather than any structural distortion of the magnitude listed in Table I.

IV. CONCLUSIONS

In investigating a possible structural origin to uniaxial magnetic anisotropy arising from an in-plane distortion of an iron film at the interface to a gallium arsenide substrate, we have examined iron films of thickness 2 and 5 monolayers using polarization-dependent XAFS. Both structural and electronic anisotropies were observed for the 2 ML film, with the difference in nearest-neighbor distances being 0.02(1) Å—a factor of 3 smaller than predicted by first principles calculations, but consistent with having distances along the ⟨−110⟩ direction larger than along the ⟨110⟩. Anisotropy in the mean-square-relative-displacements is present for the 5 ML, with more disorder indicated for the ⟨110⟩ direction, but any structural distortion as evidenced by differences in nearest-neighbor distances between the ⟨110⟩ and ⟨−110⟩ directions of the film was less than error.

ACKNOWLEDGMENTS

This research was supported by NSERC. PNC/XOR facilities at the Advanced Photon Source, and research at these facilities, are supported by the U. S. Department of Energy–Basic Energy Sciences, a major facilities access grant from NSERC, the University of Washington, Simon Fraser University, the Pacific Northwest National Laboratory, and the Advanced Photon Source. Use of the Advanced Photon Source is also supported by the U. S. Department of Energy, Office of Science, Office of Basic Energy Sciences, under Contract No. W-31-109-Eng-38.

[1] G. Wastlbauer and J. A. C. Bland, Adv. Phys. **54**(2), 137 (2005). This work is a comprehensive review of the Fe/GaAs system up to and including 2004. Many of the references cited below can also be found here. We have opted not to include this reference every time we needed to cite a work, but the reader can assume that some additional useful information is likely present in this review.

[2] F. Monteverde, A. Michel, J.-P. Eymery, and Ph. Guérin, J. Cryst. Growth **267**, 231 (2004).

[3] G. Wolterdorf, M. Buess, B. Heinrich, and C. H. Back, Phys. Rev. Lett. **95**, 037401 (2005).

[4] T. A. Moore, M. J. Walker, A. S. Middleton, and J. A. C. Bland, J. Appl. Phys. **97**, 053903 (2005).

[5] T. Manago, M. Mizuguchi, and H. Akinaga, J. Cryst. Growth **237**, 1378 (2005).

[6] A. Brambilla, L. Duò, M. Cantoni, M. Riva, R. Bertacco, M. Portalupi, and F. Ciccacci, Solid State Commun. **135**, 158 (2005).

[7] T. A. Moore, S. M. Gardiner, C. M. Guertler, and J. A. C. Bland, Physica B **343**, 337 (2004).

[8] J. S. Claydon, Y. B. Xu, M. Tselepi, J. A. C. Bland, and G. Van der Laan, Phys. Rev. Lett. **93**, 037206 (2004).

[9] L. Giovanelli, C.-S. Tian, P. L. Gastelois, G. Panaccione, M. Fabrizioli, M. Hochstrasser, M. Galaktionov, C. H. Back, and G. Rossi, Physica B **345**, 177 (2004).

[10] L. Giovanelli, G. Panaccione, G. Rossi, M. Fabrizioli, C. S. Tian, P. L. Gastelois, J. Fujii, and C. H. Back, Phys. Rev. B **72**, 045221 (2005).

[11] R. Moosbühler, F. Bensch, M. Dumm, and G. Bayreuther, J. Appl. Phys. **91**, 8757 (2002).

[12] E. M. Kneedler, B. T. Jonker, P. M. Thibado, R. J. Wagner, B. V. Shanabrook, and L. J. Whitman, Phys. Rev. B **56**, 8163 (1997).

[13] T. L. Monchesky, B. Heinrich, R. Urban, K. Myrtle, M. Klaua, and J. Kirschner, Phys. Rev. B **60**, 10242 (1999).

[14] F. Bensch, G. Garreau, R. Moosbühler, G. Bayreuther, and E. Beaurepaire, J. Appl. Phys. **89**, 7133 (2001).

[15] M. Doi, B. Roldan Cuenya, W. Keune, T. Schmitte, A. Nefedov, H. Zabel, D. Spoddig, R. Meckenstock, and J. Pelzl, J. Magn. Magn. Mater. **240**, 407 (2002).

[16] S. McPhail, C. M. Gürtler, F. Montaigne, Y. B. Xu, M. Tselepi, and J. A. C. Bland, Phys. Rev. B **67**, 024409 (2003).

[17] W. Kipferl, M. Sperl, T. Hagler, R. Meier, and G. Bayreuther, J. Appl. Phys. **97**, 10B313 (2005).

[18] R. A. Gordon, E. D. Crozier, D.-T. Jiang, T. L. Monchesky, and B. Heinrich, Phys. Rev. B **62**, 2151 (2000).

[19] R. A. Gordon, E. D. Crozier, D.-T. Jiang, P. S. Budnik, T. L. Monchesky, and B. Heinrich, Surf. Sci. **581**, 47 (2005).

[20] M. Gester, C. Daboo, R. J. Hickens, S. J. Gray, and J. A. C. Bland, Thin Solid Films **275**, 91 (1996).

[21] F. Bensch, R. Moosbühler, and G. Bayreuther, J. Appl. Phys. **91**, 8754 (2002).

[22] O. Thomas, Q. Shen, P. Schieffer, N. Tournerie, and B. Lépine, Phys. Rev. Lett. **90**, 017205 (2003).

[23] N. A. Morley, M. R. J. Gibbs, E. Ahmad, I. G. Will, and Y. B. Xu, J. Phys.: Condens. Matter **17**, 1201 (2005).

[24] N. A. Morley, S. L. Tang, M. R. J. Gibbs, E. Ahmad, I. G. Will, and Y. B. Xu, J. Appl. Phys. **97**, 10H501 (2005).

[25] J. J. Krebs, B. T. Jonker, and G. A. Prinz, J. Appl. Phys. **61**, 2596 (1987).

[26] S. Mirbt, S. Sanyal, C. Isheden, and B. Johansson, Phys. Rev. B **67**, 155421 (2003).

[27] T. L. Monchesky, A. Enders, R. Urban, K. Myrtle, B. Heinrich, X.-G. Zhang, W. H. Butler, and J. Kirschner, Phys. Rev. B **71**, 214440 (2005).

[28] T. L. Monchesky, R. Urban, B. Heinrich, M. Klaua, and J. Kirschner, J. Appl. Phys. **87**, 5167 (2000).

[29] Karl Rudolf Bauchspiess, Ph.D. thesis, Simon Fraser University, 1990. A Study of the Pressure-induced Mixed Valence Transition in SmSe and SmS by X-ray Absorption Spectroscopy.

[30] D. T. Jiang and E. D. Crozier, Can. J. Phys. **76**, 621 (1998).

[31] J. Stöhr, *in X-Ray Absorption Spectroscopy: Applications, Techniques of EXAFS, SEXAFS, and XANES*, edited by D. C. Koningsberger and R. Prins (Wiley, New York, 1988), Chap. 10.

[32] H. Oyanagi, K. Sakamoto, R. Shioda, Y. Kuwahara, and K. Haga, Phys. Rev. B **52**, 5824 (1995).

[33] P. L. Le Fevre, H. Magnan, O. Heckmann, V. Brios, and D. Chandesris, Phys. Rev. B **52**, 11462 (1995).

[34] E. D. Crozier, Nucl. Instrum. Methods Phys. Res. B **133**, 134 (1997).

[35] S. M. Heald, D. L. Brewe, E. A. Stern, K. H. Kim, F. C. Brown, D. T. Jiang, E. D. Crozier, and R. A. Gordon, J. Synchrotron Radiat. **6**, 347 (1999).

[36] R. A. Gordon, E. D. Crozier, J. Shoults, and D.-T. Jiang, Rev. Sci. Instrum. **73**, 2849 (2002).

[37] J. O. Cross and A. I. Frenkel, Rev. Sci. Instrum. **70**, 38 (1999).

[38] M. Newville, P. Livins, Y. Yacoby, J. J. Rehr, and E. A. Stern, Phys. Rev. B **47**, 14126 (1993).

[39] E. D. Crozier, A. J. Seary, M. K. McManus, and D. T. Jiang, J. Phys. IV **7**, C2 (1997).

[40] S. I. Zabinsky, J. J. Rehr, A. Ankudinov, R. C. Albers, and M. J. Eller, Phys. Rev. B **52**, 2995 (1995).

[41] T. Ressler, J. Phys. IV **7**, C2 (1997).